It is understood in the above discussion that $\dot{m}$ is to be interpreted as the actual mass flow rate through the duct. Then, as will be shown, various approximations to the solution will give rise to various approximations to the throat radius to accommodate that mass flow. This procedure is different from that used by Hall and others who keep the nozzle throat radius fixed and obtain various approximations to the mass flow. However, the use of the stream function as an independent variable suggests the procedure used here.

It would appear that before Eqs. (25) and (27) are solved for V_1^* and ϕ_1, the quantity $a^*(\eta)$ would have to be specified and that $\zeta_0(\eta)$ be determined from Eq. (22). Fortunately, this is not the case since η can be eliminated from Eqs. (25) and (27) with the $\zeta_0(\eta)$ relation given by Eq. (22) thus yielding

$$2V_1^*\partial V_1^*/\partial\xi - \partial\phi_1/\partial\zeta_0 - (1/\zeta_0)\phi_1 = 0 \tag{35}$$

and

$$\partial\phi_1/\partial\xi = \partial V_1^*/\partial\zeta_0 \tag{36}$$

where the boundary conditions on $\phi_1(\xi,\zeta_0)$ are $\phi_1(\xi,0) = 0$ and $\phi_1(\xi,1) = \xi$. These equations are similar to the first approximation equations of Hall [Eqs. (73) and (74) of Ref. 2] and their solution gives

$$V_1^* = \tfrac{1}{2}\zeta_0^2 - \tfrac{1}{4} + \xi \tag{37}$$

$$\phi_1 = \tfrac{1}{4}\zeta_0^3 - \tfrac{1}{4}\zeta_0 + \zeta_0\xi \tag{38}$$

Transforming from ξ,η to ξ,ζ_0 coordinates in Eqs. (26) and (28) with the aid of Eq. (22) gives for the second approximation

$$2V_1^*(\partial V_2^*/\partial\xi) + (2V_2^* + V_1^{*2})(\partial V_1^*/\partial\xi) + \phi_1\partial\phi_1/\partial\xi - \partial\phi_2/\partial\zeta_0 - (2-\gamma)V_1^*(\partial\phi_1/\partial\zeta_0) - 1/\zeta_0[\phi_2 + (2-\gamma)V_1^*\phi_1] = 0 \tag{39}$$

$$\phi_1\partial V_1^*/\partial\xi + \partial\phi_2/\partial\xi + V_1^*(\partial\phi_1/\partial\xi) = \partial V_2^*/\partial\zeta_0 \tag{40}$$

where the boundary conditions on $\phi_1(\xi,\zeta_0)$ are $\phi_2(\xi,0) = 0$ and $\phi_2(\xi,1) = 0$. Following the procedure used by Hall, the solution for the second approximation terms is found to be

$$V_2^* = \frac{2\gamma+9}{24}\zeta_0^4 - \frac{4\gamma+15}{24}\zeta_0^2 + \frac{10\gamma+57}{288} + \xi\left(\zeta_0^2 - \frac{5}{8}\right) - \frac{2\gamma-3}{6}\xi^2 \tag{41}$$

$$\phi_2 = \frac{8\gamma+15}{72}\zeta_0^5 - \frac{20\gamma+45}{96}\zeta_0^3 + \frac{28\gamma+75}{288}\zeta_0 + \left(\frac{4\gamma+9}{12}\right)(\zeta_0^3 - \zeta_0)\xi \tag{42}$$

This is similar in form to Hall's second solution [Eqs. (77) and (78) of Ref. 2]. To complete the second order solution, the second order approximation to the radius must be determined. Changing variables with the aid of Eq. (22), Eq. (24) can be written

$$\zeta_2 = \left(\frac{\gamma+1}{2}\right)\frac{1}{\zeta_0}\int_0^{\zeta_0} V_1^*\zeta_0 d\zeta_0 \tag{43}$$

Using Eq. (37) for V_1^* and performing the integration in the above equation, Eq. (21) for the radial coordinate becomes

$$\zeta = \zeta_0 + [(\gamma+1)/6]1/\zeta_0[(\xi - \tfrac{1}{4} + \tfrac{1}{2}\zeta_0^2)^3 - (\xi - \tfrac{1}{4})^3]\epsilon^2 + \ldots \tag{44}$$

which at the wall ($\zeta_0 = 1$) becomes

$$\zeta_w = 1 + \{(\gamma+1)/192 + [(\gamma+1)/4]\xi^2\}\epsilon^2 + \ldots \tag{45}$$

It is seen that this equation is in accord with Eq. (33). In situations where the second order solution adequately describes the solution the throat radius would be taken as

$$r_t = \{1 + [(\gamma+1)/192]\epsilon^2\}r_{t_o} \tag{46}$$

Conclusions

A first and second order solution of the transonic equations for nonuniform total energy has been obtained using the stream function as an independent variable. Neither the first solution expressed by Eqs. (37) and (38) nor the second solution expressed by Eqs. (41) and (42) is explicitly dependent upon $a^*(\eta)$. Hence, the dimensionless quantities V^*, ϕ and the sonic line shape are formally independent of any existing variation in the total temperature. However, the details of the rotational flowfield such as the distributions of a, ρ and V are dependent upon $a^*(\eta)$.

References

[1] Sauer, R., "General Characteristics of the Flow Through Nozzles at Near Critical Speeds," TM 1147, June 1947, NACA.

[2] Hall, I. M., "Transonic Flow in Two-Dimensional and Axially Symmetric Nozzles," *Quarterly Journal of Mechanics and Applied Mathematics*, Vol. XV, Pt. 4, 1962, pp. 487–508.

[3] Hopkins, D. F. and Hill, D. E., "Effect of Small Radius of Curvature on Transonic Flow in Axisymmetric Nozzles," *AIAA Journal*, Vol. 4, No. 8, Aug. 1966, pp. 1337–1343.

[4] Kliegel, J. R. and Quan, V., "Convergent–Divergent Nozzle Flows," *AIAA Journal*, Vol. 6, No. 9, Sept. 1968, pp. 1728–1734.

[5] Kliegel, J. R. and Levine, J. N., "Transonic Flow in Small Throat Radius of Curvature Nozzles," *AIAA Journal*, Vol. 7, No. 7, July 1969, pp. 1375–1378.

Probe Geometry Effects on Turbulent Plasma Diagnostics

A. K. Ghosh* and C. Richard†

RCA Limited Research Laboratories, Montreal, Canada

In recent years, the cylindrical electrostatic probes have been most extensively used for turbulent plasma diagnostics.[1–6] The object is to determine the statistics of electron density fluctuations in turbulent plasmas with high-spatial resolution. In this Note, we report some studies on the perturbing effects of the probe geometry on the turbulent plasma parameters when they are used to measure the local statistical properties of turbulent plasma flows. The effects studied are: 1) frequency filtering effects of the cylindrical electrostatic probes on the power-frequency spectrum when placed axially along the turbulent plasma flow. 2) The "wake" effect of an upstream probe on a downstream probe when the pair is used to measure various statistical moments of the turbulent plasma flow.

A vortex-stabilized argon arc (100 amp at 20 v) has been used as a plasma source[4] which opens into an evaucated test section (3.5 ft diam, 5 ft long) through a nozzle. The typical operating pressure in the arc chamber is 150 torr and the test section pressure is 3 torr. The plasma jet flows into the test section as an extended plume which can be run into the turbulent mode by varying the gas flow rate.

Received January 15, 1971; revision received May 10, 1971. The work was supported by the Defense Research Board of Canada. The authors wish to acknowledge illuminating discussions with T. W. Johnston, I. P. Shkarofsky, and A. I. Carswell during the progress of this work.

Index categories: Plasma Dynamics and MHD; Research Facilities and Instrumentation.

* Member of Scientific Staff.

† Chercheur, Institut de Recherche de l'Hydro-Quebec, Varennes, Quebec, Canada.

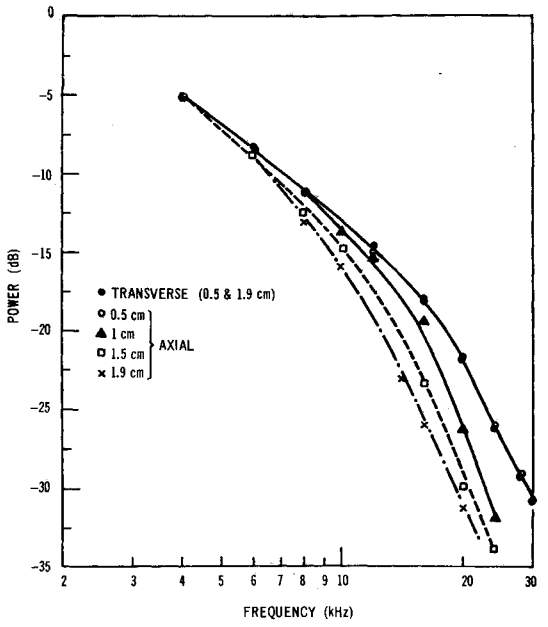

Fig. 1 Power-frequency spectra as seen by probes of different lengths placed axially along the flow.

Frequency Filtering Effect

When an electrostatic probe (cylindrical) of some finite length is immersed into a turbulent flowing plasma, the power-frequency spectrum as measured by the probe will be different[8] from the actual spectrum due to averaging of the eddies over the probe length. The effect of such averaging is to introduce a rapid fall off in the spectrum similar to the effect of a low-pass filter.

To check this, cylindrical electrostatic probes (biased to collect ion saturation current) of different lengths (5–20 mm) but the same diameter (0.2 mm) are mounted on a movable assembly in an array. Their positions and orientations can be adjusted with respect to the plasma flow direction.

Our experimental results (Fig. 1) show that when the probes are transverse to the flow, the spectra, as measured by different length probes at the same location are identical indicating there is no significant filtering effect. However, when the probes are placed axially along the flow the spectra show a significant change. The transverse probe spectra may be considered as the unfiltered spectrum and the filtered characteristics of different axial probes can be determined by subtracting their rapidly falling spectra from the unfiltered spectrum. The cut-off frequency is defined by the frequency corresponding to the point where the asymptote to the filter frequency response characteristics beyond the pass band intersects the OdB line. This is illustrated in Fig. 2a. The cut-off frequency is found to vary linearly (Fig. 2) with the inverse of probe length. The slope of the curve is found to be half the measured flow velocity ($v = 2.5 \times 10^4$ cm/sec) so that the cut-off frequency is given by

$$f_c = v/2L \qquad (1)$$

This indicates that averaging of the eddies starts when the wavelength of the eddy is half the probe length. This result is in agreement with similar investigations[7] of the resolution length of the hot wire anemometer probe in non-ionized turbulent flow. Qualitative measurements of spectra for different orientations of a 2-cm probe indicate that the cut-off condition is determined by the projection of the probe length along the flow.

Wake or Shadow Effect

Another effect studied is the "wake" effect of an upstream probe on a downstream probe when the pair or an array is used to measure axial electron density profiles and the longitudinal space time correlation function. In the first set of investigations using a pair of probes, the downstream probe (0.2 mm diam) is rotated about the upstream probe (0.4 mm diam) in a half circle at different separations (3–40 mm). When the probes are very close and on axis in the same line of flow, the downstream probe is in the wake of the upstream probe. The average and rms ion probe currents [i.e. $\bar{n}_e$ and $\delta(n_e^2)^{1/2}$] as seen by the downstream probe are expected to be smaller than if the upstream probe is not present. The reasons for the expected decrease in the downstream probe current when it is in the shadow of the upstream probe may be the following: 1) The upstream probe acts like a recombination surface for the electrons and positive ions and thus depleting the electron and ion density in its vicinity. 2) The upstream probe may trigger local turbulence as an obstacle and thus modifying the local statistics of plasmas. If the downstream probe is rotated slightly off-axis the probe currents tend to increase as it is going out of the wake. At some larger separations the wake effect becomes more and more insignificant and the current collected by the downstream probe for different angles (θ) is influenced by the radial and axial density profiles in the jet. Figure 3 illustrates this wake effect (at flow velocity 1.7×10^4 cm/sec) on the average electron densities normalized with respect to the upstream fixed probe of 0.4 mm diam, as seen by a 0.2-mm-diam downstream probe. The "wake" effect is also found to affect the velocity and longitudinal space correlation measurements. The results show that at small separations, the upstream probe tends to slow down the plasma flow and the longitudinal correlation function shows a "dip." The apparent slowing down effect of the flow has also been observed by other workers.[8] Similar

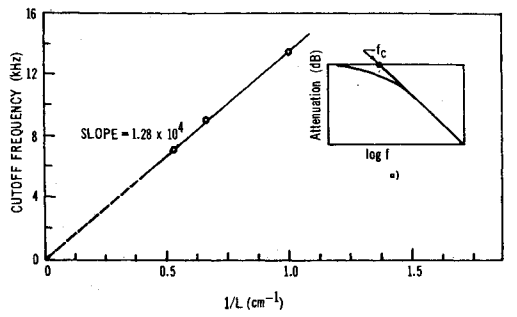

Fig. 2 Variation of cutoff frequency with reciprocal of the probe length. Insert "a" illustrates the definition of cut-off frequency.

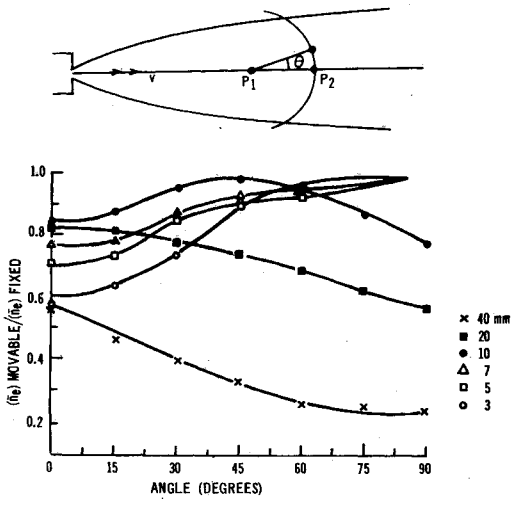

Fig. 3 Variation of $(\bar{n}_e)_{\text{movable}}/(\bar{n}_e)_{\text{fixed}}$ with θ for 0.4-mm (diam) upstream (fixed) probe and 0.2-mm (diam) downstream (movable) probe; a schematic of the probe positions is also shown.

measurements for 0.625-mm- and 0.125-mm-diam upstream probes show that the wake effect is more pronounced in the former case and insigificant for the latter under similar plasma flow conditions mentioned previously.

These investigations indicate that the size and the orientation of a cylindrical probe may affect the measurements of the turbulent properties of a flowing plasma. The wake effect may be avoided using small diameter probes. However, since a very small diameter probe when used in a high temperature plasma jet gets red hot, the absolute electron density determination needs calibration procedure. In ballistic ranges, on the other hand, since the measuring time is short, a very small diameter probe can be used.

References

[1] Demetriades, A. and Doughman, E. L., "Langmuir Probe Diagnostics of Turbulent Plasmas," *AIAA Journal*, Vol. 4, No. 3, 1966, pp. 451–460.

[2] Guthard, H., Weissman, D. E., and Morita, T., "Measurements of the Charged Particles of an Equilibrium Turbulent Plasma," *The Physics of Fluids*, Vol. 6, 1965, pp. 1766–1772.

[3] Granatstein, V. L., "Structure of Wind Driven Plasma Turbulence as Resolved by Continuum Ion Proces," *The Physics of Fluids*, Vol. 10, 1967, pp. 1236–1244.

[4] Johnston, T. W. et al., "Correlation Studies in Neutral-Dominated Plasma Turbulence," Proceedings of the Symposium on Turbulence of Fluids and Plasmas, Vol. XVIII, 1968.

[5] Heckman, D., Tardiff, L., and Lahaye, C., "Experimental Study of Turbulent Wakes in the CARDE Free-Flight Ranges," *Proceedings of the Symposium on Turbulence of Fluids and Plasmas*, Vol. XVIII, 1968.

[6] Ghosh, A. K., Richard, C., and Johnston, T. W., "Correlation Between Ion and Electron Probe Currents in Turbulent Plasma Flow," *Canadian Journal of Physics*, Vol. 49, 1971, pp. 1114-1119.

[7] Hinze, J. O., *Turbulence*, McGraw-Hill, New York, 1959.

[8] Fox, J., "Space Correlation Measurements in the Fluctuating Turbulent Wakes behind Projectiles," *AIAA Journal*, Vol. 5, No. 2, Feb. 1968, pp. 233–238.

Oscillations in Digital Control Systems

CHARLES L. PHILLIPS* AND JOHN C. JOHNSON†
Auburn University, Auburn, Ala.

AND

DARREL L. CHENOWETH‡
University of Louisville, Louisville, Ky.

Introduction

A PROBLEM in the implementation of digital controllers is the generation of low-amplitude oscillations by signal quantization. It has been shown[1] that if a digital control system is stable in a bounded-input bounded-output sense with no quantization, then the system will be stable in the same sense with quantization, provided that the controller operates with fixed-point arithmetic. However, it is well known that oscillations with bounded amplitudes may occur in such systems. An investigation of these oscillations is presented in this Note.

Development

The effects of quantization may be considered as a nonlinear gain, where this gain is a function of the signal being quantized. Consider a linear discrete system in which the effects of quantization are ignored.

$$\mathbf{x}(k+1) = A\mathbf{x}(k) + B\mathbf{u}(k) \tag{1}$$

With quantization present, this system may be modeled as

$$\mathbf{x}(k+1) = A_Q\mathbf{x}(k) + B_Q\mathbf{u}(k) \tag{2}$$

where, in general, A_Q and B_Q are nonlinear functions of the states and the inputs. Or,

$$A_Q = A_Q[\mathbf{x}(k),\ \mathbf{u}(k)] \tag{3}$$

$$B_Q = B_Q[\mathbf{x}(k),\ \mathbf{u}(k)] \tag{4}$$

A cause of low-amplitude oscillations in the system described by Eqs. (1) and (2) will now be investigated. Consider that the signal into one quantizer has settled into a certain quantization level for at least several consecutive sampling instants. Suppose that the system is modeled such that the signal out of this quantizer is $x_i(k)$. Then, for the several sampling instants,

$$x_i(k+1) = x_i(k) = x_i \tag{5}$$

The ith equation of Eq. (2) will be now Eq. (5). Thus, Eq. (2) can be written as

$$\mathbf{x}(k+1) = A_q\mathbf{x}(k) + B_q\mathbf{u}(k) + A_1\mathbf{x} = A_q\mathbf{x}(k) + [A_q, B_q]\begin{vmatrix}\mathbf{x}\\ \mathbf{u}(k)\end{vmatrix} \tag{6}$$

The matrices A_q and B_q can be obtained from A_Q and B_Q by considering the quantizer in question to be open. The matrix A_1 can be obtained by considering the output of this quantizer to be a source x_i, and ignoring the effects of $x_j(k), j \neq i$, and $\mathbf{u}(k)$ on $\mathbf{x}(k+1)$, since these effects are included in A_q and B_q. Thus, in A_1 all columns are zero vectors except the ith column. The matrices are illustrated in the example below.

If A_q in Eq. (6) represents an unstable system, the input into the quantizer cannot remain within the quantization level for an indefinite period. For this case, with the systems inputs constant over a long period of time, the system states cannot settle to constant values, but instead will exhibit oscillations. These oscillations will be present whether fixed-point or floating-point arithmetic is used. The amplitude of the oscillations will, of course, depend on the digital word-lengths used within the controller.

Example

Consider the discrete model of the stable digital control system shown in Fig. 1. In this figure, the blocks that con-

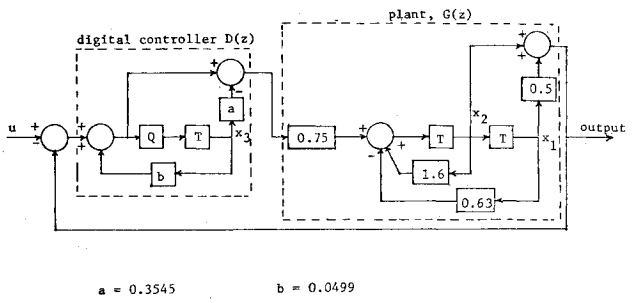

Fig. 1 Digital control system.

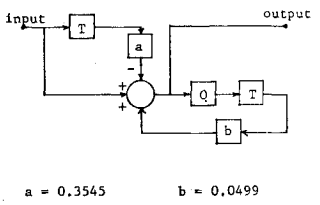

Fig. 2 Controller with direct programing form.

Received April 19, 1971, revision received June 25, 1971. This research was supported by Marshall Space Flight Center, Huntsville, Ala. under contract NAS 8-11274.

* Professor, Department of Electrical Engineering.

† Research Associate, Department of Electrical Engineering.

‡ Assistant Professor.